Diastereomeric Selective Effects for Growth Inhibition of Synthesized Mini Parallel Double-Stranded Peptides on *Escherichia coli* and *Staphylococcus aureus*

Shigeki KOBAYASHI,*[,a] Nahomi ATUCHI,[a] Hiroki KOBAYASHI,[a] Akiko SHIRAISHI,[b] Hajime HAMASHIMA,[b] and Akira TANAKA[a]

[a] *Department of Analytical Chemistry of Medicines, Showa Phamaceutical University; and* [b] *Department of Microbiology, Showa Phamaceutical University; 3–3165 Higashi-tamagawagakuen, Machida, Tokyo 194–8543, Japan.*

Received September 8, 2003; accepted November 7, 2003

The synthesis of a series of mini double-stranded peptides containing chiral–x-Phe–y-Phe–peptide residues and the diastereomeric selective effects of these compounds on *Escherichia coli* NIHJ JC-2 and *Staphylococcus aureus* FDA 209P growth are described. In the case of bis(y-Phe–x-Phe)-*N*,*N*-ethane-1,2-diamine, bis(y-Phe–x-Phe)-*N*,*N*-buthane-1,4-diamine, bis(y-Phe–x-Phe)-*N*,*N*-hexane-1,6-diamine, and bis(y-Phe–x-Phe)-*N*,*N*-dodecane-1,12-diamine, *etc.*, the four configurations, (L-, L-), (D-, L-), (L-, D-) and (D-, D-), where the symbols x- and y- represent optical isomers with L- and D- forms, were used to investigate the relationship between chirality and antibacterial activity. The level of activity increased in the following order: (L-, L-)<(D-, D-)<(L-, D-)<(D-, L-). The data show that (D-, L-) chilarity is more potent than (L-, L-) chilarity. Then, these results suggest that the –y-Phe–x-Phe Phe–sequence in the double-stranded peptide has anti-bacterial activity and the chirality of –y-Phe–x-Phe affects the anti-bacterial activity. Our results show that the uptake by penetration through the membrane of bis(y-Phe–x-Phe)$_2$-Spacers is a first step in the expression of anti-bacterial activity. This study provides new insights in the chirality-antibacterial activity relationships of a series of mini double-stranded peptides.

Key words peptide; diastereomer; chirality; antibacterial activity; log P; circular dichroism

The function of proteins and enzymes is much related to the tertiary structure formed with the folding of secondary structures, *e.g.*, the α-helix, β-sheet, or β-turn. Although β-sheet or β-turn structures are found in peptides and proteins, their biological functions are poorly understood yet compared with the α-helix. In an effort to clarify the chemical properties, functions, and stereochemistry of β-turn (or β-hairpin) and antiparallel β-sheet structures, the design and synthesis of peptides have been reported by a number of research groups.[1—6] Model compounds which mimic β-sheet and β-turn structures have been shown to adopt β-hairpin structures in an aqueous solution, and hydrogen bonding can stabilize the β-turn structure. Recently, we have reported the synthesis and chemical properties of mini parallel double-stranded peptides, (L-AA^3–L-AA^2–L-AA^1)$_2$-spacer(S) (AA=amino acids; S=ethano- and dodecano-, *etc.*) conjugated two peptide strands to a mini loop (=spacer).[7] Especially, the chemical properties of bis(L-Leu–L-Phe–L-Phe)-*N*,*N*-ethane-1,2-diamine and bis(L-Leu–L-Phe–L-Phe)-*N*,*N*-dodecane-1,12-diamine mediated β-sheet-like conformation were described in the previous paper because the sequences like –Phe–Phe–, –Leu–Phe–Phe–, and –Val–Phe–Phe– which are little existence in natural peptides and proteins. Moreover, the –Val–Phe–Phe–, interestingly, is contained in Alzheimer's disease related β-amyloid peptide (Aβ).

The aims of the present study are the synthesis of double-stranded peptides containing chiral –x-Phe–y-Phe– sequences and elucidation of the structure–activity relationship between antibacterial activity and chirality of the –Phe–Phe– sequence. We synthesized four chiral types, –L-Phe–L-Phe–, –D-Phe–L-Phe–, –L-Phe–D-Phe– and –D-Phe–D-Phe– of bis(y-Phe^2–x-Phe^1)-*N*,*N*-hexane-1,6-diamine and examined the effect of chirality on the growth inhibition of *Escherichia coli* NIHJ JC-2 and *Staphylococcus aureus* FDA 209P. Interestingly, the activity increased in the following order: bis(L-Phe–L-Phe)-*N*,*N*-hexane-1,6-diamine<bis(D-Phe–D-Phe)-*N*,*N*-hexane-1,6-diamine<bis(L-Phe–D-Phe)-*N*,*N*-hexane-1,6-diamine<bis(D-Phe–L-Phe)-*N*,*N*-hexane-1,6-diamine. Compound bis(D-Phe–L-Phe)-*N*,*N*-hexane-1,6-diamine is about 32 times more active than bis(L-Phe–L-Phe)-*N*,*N*-hexane-1,6-diamine. A similar trend was seen in the order of the activity for double-stranded peptides with a spacer of carbon number $n=2$, 4, 8, and 12. This result shows that the antibacterial activity is affected by the diastereomeric selectivity of Phe in double-stranded peptides. The biological potency of D-Phe–L-Phe– or –L-Phe–D-Phe– sequences may play an important role in antibacterial activity or cytotoxicity. What is the biological role of the configurations (D-, L-) and (L-, D-) in the y-Phe–x-Phe sequence? The mechanisms of action may be similar to those of antibacterial peptides such as gramisidine A. In order to elucidate the mechanism of interaction of these double-stranded peptides with cell membrane, we synthesized a new fluorescence probe bis(Dns–L-Phe)-*N*,*N*-ethane-1,2-diamine (Dns=dansyl group) conjugated to dansyl chloride to the N-terminus of bis(L-Phe)-*N*,*N*-ethane-1,2-diamine. Fluorescence microscopy showed that the probe was taken up into the cytosol and passed through the membrane of A 431 cells. Bis(D-Phe–L-Phe)-*N*,*N*-hexane-1,6-diamine, *etc.* may also form pores which pass ions. This indicates that double-stranded peptides pass through the cell membrane (or bacterial cell wall). It suggests that compounds bis(D-Phe–L-Phe)-*N*,*N*-hexane-1,6-diamine, *etc.* form chiral pores on the membrane of bacteria or cells.

Finally, we found that the major and minor action groups can be seen in double-stranded peptides, bis(y-Phe–x-Phe)-*N*,*N*-buthane-1,4-diamine and bis(y-Phe–x-Phe)-*N*,*N*-hexane-1,6-diamine, *etc.*, and the (D-, L-) or (L-, D-) forms of the minor action group act as diastereomeric selective inhibitors

* To whom correspondence should be addressed. e-mail: kobayasi@ac.shoyaku.ac.jp

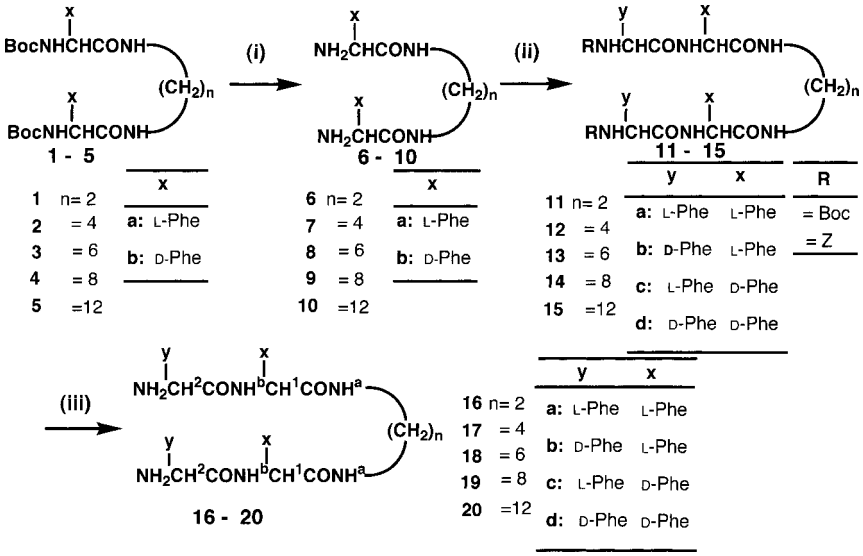

Reagents: (i) TFA at 4 °C. (ii) CDI, Boc-AA-OH (AA=amino acid), dry $CHCl_3$. (iii) TFA at 4 °C (or 5% Pd/C, H_2, DMF/CH_3OH for *Z*-deprotection). *b*) **14c**=*Z* protect compound.

Chart 1

of the growth of *E. coli* NIHJ JC-2 and *S. aureus* FDA 209P. Thus this is the first investigation of the diastereomeric selective effects and structure–activity relationship for the antibacterial activity of a series of new mini double-stranded peptides.

Results

Synthesis and Characterization by CD and NMR A series of double-stranded peptides, bis(y-Phe–x-Phe)-*N*,*N*-ethane-1,2-diamine (**16a**—**d**) and bis(y-Phe–x-Phe)-*N*,*N*-dodecane-1,12-diamine (**20a**—**d**), were synthesized by the methods described in the previous paper.[7] The four optical isomers of bis(y-Phe–x-Phe)-*N*,*N*-buthane-1,4-diamine (**17a**—**d**) and bis(y-Phe–x-Phe)-*N*,*N*-hexane-1,6-diamine (x, y=L- or D-form) (**18a**—**d**), were prepared as shownin Chart 1 and their chemical properties and circular dichroism (CD) were compared. bis(L-Phe)-*N*,*N*-hexane-1,6-diamine (**8a**) was treated with C-terminal activated Boc–L-PheOH prepared using *N*,*N*′-carbonyldiimidazole (CDI) in dry $CHCl_3$ to provide bis(Boc–y-Phe–x-Phe)-*N*,*N*-hexane-1,6-diamine (**13a**). The crude reaction mixtures were purified by silica gel column chromatography. The Boc- and *Z*-protecting groups were removed with trifluoroacetic acid (TFA) in an ice bath and by hydrogenation in the presence of 5% Pd/C in DMF/MeOH solution, respectively. The resulting free bases were purified with an overall yield of about 30 to 40% by recrystallization or silica gel column chromatography, and satisfactory results were obtained by thin layer (TLC, silica gel) or reverse-phase high performance liquid chromatography (HPLC). Interestingly, the *Rf* values of Boc forms on TLC, contrary to expectation, increased in the following order: **6a**<**7a**<**8a**<**9a**<**10a**. Compounds bis(L-Phe)-*N*,*N*-buthane-1,4-diamine (**7a**) (*Rf*=0.06) and bis(L-Phe)-*N*,*N*-octane-1,8-diamine (**9a**) (*Rf*=0.16) have larger *Rf* values than bis(L-Phe–L-Phe)-*N*,*N*-butane-1,4-diamine **17a** (*Rf*=0.41) and bis(L-Phe–L-Phe)-*N*,*N*-octane-1,8-diamine (**19a**) (*Rf*=0.43), respectively. Moreover, the *Rf* of compound **17a** is larger than that of the diastereomers, bis(D-Phe–L-Phe)-*N*,*N*-butane-1,4-diamine **17b** (*Rf*=0.16) and bis(L-Phe–D-Phe)-*N*,*N*-butane-1,4-diamine **17c** (*Rf*=0.16), as listed in Table 1. The *Rf* values in these compounds are proportional to the carbon number (*n*) of the polyamines spacer and the chirality. Compounds **17b** and **17c**, *etc.* have higher polarity than the diastereomers, **17a** and **17d**, moreover, similar trends were observed for the other double-stranded peptides.

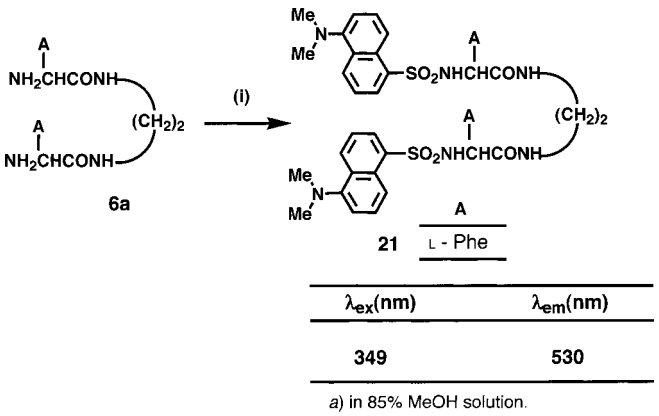

Reagents: (i) Dansyl chloride, Na_2CO_3, acetone at 4 °C.

Chart 2

In order to clarify the chemical properties, a novel fluorescence probe, bis(Dns–L-Phe)-*N*,*N*-ethane-1,2-diamine **21** conjugated dansyl group (=Dns) to N-terminus of bis(L-Phe)-*N*,*N*-ethane-1,2-diamine **6a** was synthesized as shown in Chart 2. In fluorometry, compound **21** emits a siganal at about 530 nm with an excitation wavelength of 349 nm in 85% methanol. Table 2 shows the chemical shift (δ ppm) and $^3J_{\alpha H,NH}$ coupling constants of two protons, αH^1 and αH^2, of **17a**—**d**, **18a**—**d**, and **19a**, **b**, **d** with the numbering shown in Chart 1. The chemical shifts of αH^1 and αH^2 of **18a** showed *dd* (or *ddd*) and *dd* patterns at 4.64 and 3.51 ppm, and that of **19a** appeared at 4.63 and 3.51 ppm, respectively in DMSO-d_6/$CDCl_3$ (volume ratio=0.2 ml/0.5 ml). However, the chemi-

cal shifts of αH^1 and αH^2 of the long molecule **20a** appeared at 4.50 and 4.09 ppm, respectively. The CD profiles of the bis(y-Phe–x-Phe)-*N*,*N*-hexane-1,6-diamine, **18a**—**d** (a), bis(x-Phe)-*N*,*N*-octane-1,8-diamine, **9a**—**b**, and (y-Phe–x-Phe)-*N*,*N*-octane-1,8-diamine, **19a** and **19d** exhibit a mirror image as shown in Fig. 1, and they are pure stereo-chemically. The molar ellipticity ([θ]) of compounds **9a** and **9b** is smaller in intensity than that of **19a** or **19d** conjugated to four Phe. The CD curve of **18b**, a diastereomer of **18a**, is obviously a mirror image of **18c**, and the [θ] intensity is small compared with **18a** or **18d**. The positive maxima of CD at 228 and 234 nm of **18b** differ from the positive maximum at 224 nm of **18a**, which may be related to the difference in electronic state of –L-Phe–L-Phe– and –D-Phe–L-Phe– sequences.

Table 1. TLC *Rf* Values of Some Double-Stranded Peptides Conjugated –y-Phe–x-Phe– Sequence to Spacer

Compounds	Carbon number (*n*) of spacer	Configuration	$Rf^{a,b)}$
16a	2	(L-, L-)	0.36
16c	2	(L-, D-)	0.15
17a	4	(L-, L-)	0.41
17c	4	(L-, D-)	0.16
18a	6	(L-, L-)	0.42
18c	6	(L-, D-)	0.21
19a	8	(L-, L-)	0.43
19c	8	(L-, D-)	0.31
20a	12	(L-, L-)	0.51
20c	12	(L-, D-)	0.41

a) Mean values. *b*) $CHCl_3$–MeOH (10 : 1) solvent was used for TLC development.

Table 2. Chemical Shifts of Alpha Protons and Amido Protons for Several Double-Stranded Peptides

Compounds	Chemical shift, δ (ppm)[a]				
	αH^1	αH^2	$-NH^aCO-$	$-NH^bCO-$	$^3J_{\alpha H^1,NH^b}$ (Hz)
16a	4.58	3.52	7.68	7.89	8.2
16b	4.53	3.94	7.80	8.79	7.9
16c	4.52	3.71	7.83	8.54	7.6
17a	4.63	3.50	7.58	7.94	8.6
17b	4.61	3.49	7.55	8.00	8.2
18a	4.64	3.51	7.53	7.95	8.9
18b	4.62	3.50	7.53	7.99	8.6
18c	4.63	3.50	7.52	8.00	8.5
19a	4.63	3.51	7.54	7.95	8.9
20a	4.50	4.09	7.61	8.90	8.2
20b	4.59	4.05	7.78	8.73	8.5
20c	4.61	3.49	7.45	7.95	8.2

[a]) In DMSO-d_6/$CDCl_3$ (0.2/0.5 = 0.7 ml).

Conformation in Solution We have reported that CD data, NMR data from nuclear Overhauser enhancement and exchange spectroscopy (NOESY) experiments, and *J* values of **16a** and **20a**, bis(L-Leu–L-Phe–L-Phe)-*N*,*N*-dodecane-1,12-diamine were consistent with a folded β-sheet structure.[7] Here, the experimental dihedral angles in **17a** were calculated with $^3J_{\alpha H,NH}$ values based on the coupling constant between αH and amido proton –NHCO–. In order to characterize the conformations, the values of sequential d_{NN} NOE and $d_{NH,\alpha H}$ connectivities, especially, were used. While $^3J_{\alpha H,NH}$ values for β-sheet forms fall in the range of 8 to 10 Hz, the values for α-helical forms distributed between 4 and 5 Hz.[8,9] The values indicate that **17a**, **18a**, and **19a** also adopt a β-sheet-like conformation. Figure 2 shows NOE cross peaks involving the side chains of Phe^1 and Phe^2 (*ortho*-, *meta*-, and *para*-), amido proton (–NH^aCO–), and spacer protons of **18a** and **18c** in DMSO-d_6/$CDCl_3$ (volume ratio = 0.2 ml : 0.5 ml) solution. The amido proton, NH^a, in **18a** is observed at δ 7.53. The α proton, αH^1, in **18a** is observed at δ 4.64. The coupling constants determined at 21 °C are listed in Table 2. The dihedral angles $\angle$–CO–$C^{1\alpha}$–N^b–CO– in **18a** estimated using the NMR data are about −110° since the coupling constants of NH^a and αH^1 protons in Phe^1 are $^3J_{NH^a,\alpha H^1} = 8.6$ Hz, respectively.[5]

The $^3J_{\alpha H^1,NH^b}$ data listed in Table 2 clearly show that **17a**, **18a**, and **19a** have a very similar average conformation in DMSO-d_6/$CDCl_3$ solution and have a β-sheet-like structure. However, $^3J_{\alpha H^1,NH^b}$ data for bis(D-Phe–L-Phe)-*N*,*N*-ethane-1,2-diamine **16b** and **16c** of the short spacer, C^2, support a fold-

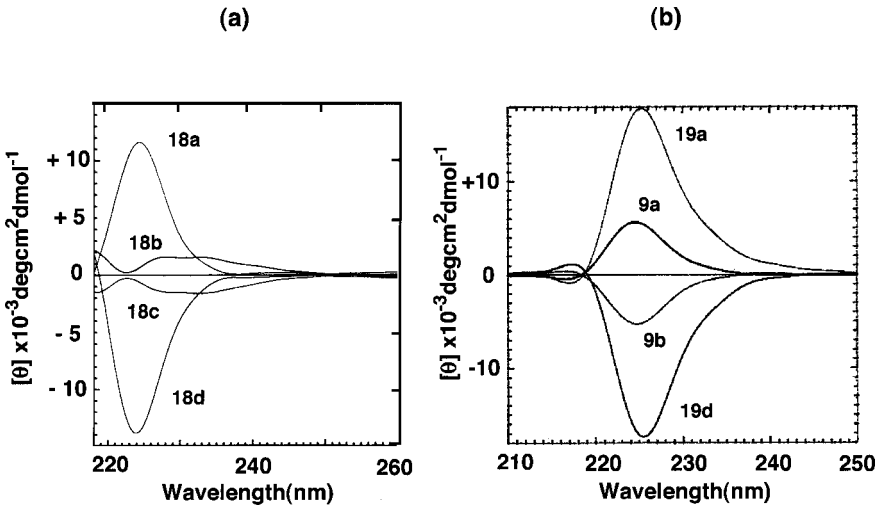

Fig. 1. Circular Dichroism Spectra for Mirror Images of Bis(y-Phe–x-Phe)-*N*,*N*-hexane-1,6-diamines **18a**—**d**, Bis(x-Phe)-*N*,*N*-octane-1,8-diamines **9a**, **b** and Bis(y-Phe–x-Phe)-*N*,*N*-octane-1,8-diamines **19a**, **d**

Concentration, **18a** (6.150×10^{-4} M), **18b** (7.462×10^{-4} M), **18c** (6.580×10^{-4} M), **18d** (5.036×10^{-4} M), **9a** (1.370×10^{-3} M), **9b** (1.187×10^{-3} M), **19a** (9.016×10^{-4} M), and **19b** (7.514×10^{-4} M) in 85% aqueous methanol employing a path length quartz cell at 22 °C. *x*-axis, λ (nm); *y*-axis, molar ellipticity [θ].

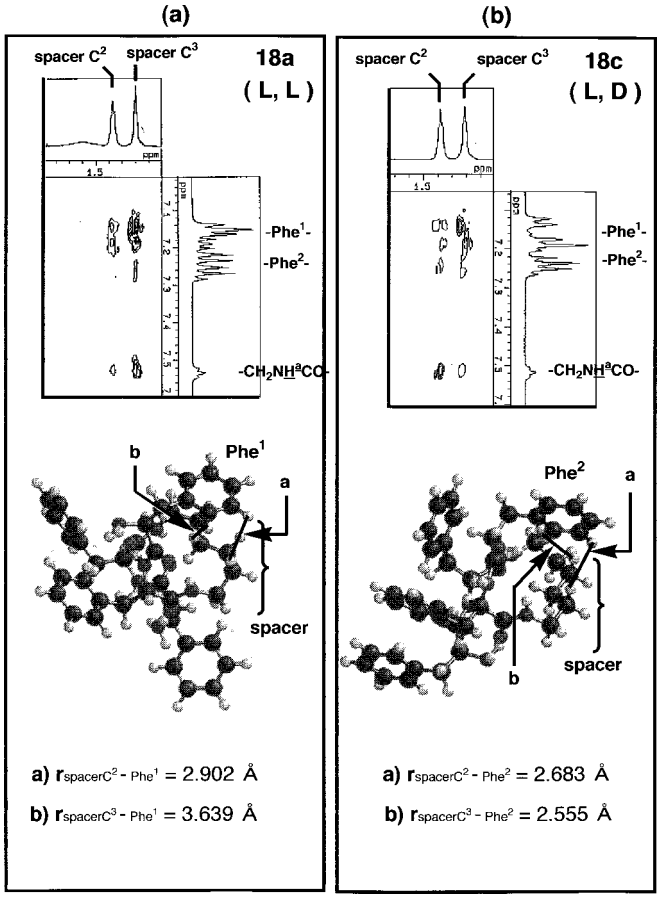

Fig. 2. NOESY Data[a] in $CDCl_3$/DMSO-d_6 (0.5 ml/0.2 ml) and Lowest Energy Conformations[b] of **18a** and **18c**

a) Showing NOEs involving the side chains of Phe[1] and Phe[2] (*ortho*-, *meta*-, *para*-), amido proton (–NH[a]CO–), and spacer protons ($C^2\times2$, $C^3\times2$). *b*) Lowest Energy Conformation of **18a** (a) and **18c** (b) obtained by a montecarlo calculation using the MMFF (molecular mechanics) Method.

ing β-sheet-like conformation more than **16a**. The NOEs between spacer protons-aromatic side chain of Phe[1] and Phe[2] in **16**—**20** also show that their distance is about 3.5—4.5 Å in the intramolecule. This suggests that the confomation is consistent with the folding structure.[7]

Calculated Conformations and Log P It may be difficult to determine which conformation is predominant in strand[1] and strand[2] of the double-stranded peptides in the intramolecule, because the compounds have an axial symmetric structure for the spacer. To understand the conformations in solution, we searched for the most stable conformation using computational chemistry. The minimum energy conformation of the double-stranded peptides was calculated by making out a conformational search with the MONTECARLO method using a MMFF94 force field (molecular mechanics). With the several conformations obtained, the minimum energy conformation was optimized with a single point energy calculation using PM3 Hamiltonian, and Log P was also calculated. Figure 2 shows several low energy conformations and the minimum energy conformation of bis(L-Phe–L-Phe)-*N*,*N*-hexane-1,6-diamine **18a** and bis(L-Phe–D-Phe)-*N*,*N*-hexane-1,6-diamine **18c**. The conformations support the experimental data obtained from the NOESY measurements. As the NOE cross peaks among Phe[1], Phe[2], and the hexano-spacer protons in bis(L-Phe–L-Phe)-*N*,*N*-hexane-1,6-diamine **18a**, are obvious, the folding conformation is confirmed. Therefore, the conformations obtained using the MONTECARLO calculations are consistent with the NOE data.

Table 3. Dipole Moment and Log P of Some Double-Stranded Peptides Conjugated –x-Phe–y-Phe– Sequence to Spacer

Compounds	Dipole moment (DM)[a] (debye)	Log P[b]
16a	6.46	2.52
16c	5.39	2.52
17a	5.20	3.08
17c	2.98	3.08
18a	1.34	3.91
18c	8.92	3.91
19a	5.53	4.75
19c	7.73	4.75
20a	2.94	6.42
20c	8.32	6.42

a) PM3 hamiltonian level. *b*) By Ghose–Crippen method.[10]

Log P is a measure of the hydrophobicity of chemicals, and was evaluated according to the method of Ghose–Crippen,[10] in our study. The results are listed in Table 3. We described in the section "Synthesis and Characterization by CD and NMR" that the *Rf* values of **16a**, **c**—**20a**, **c** on silicagel TLC increase in the following order: **16a**<**17a**<**18a**<**19a**<**20a** and **16c**<**17c**<**18c**<**19c**<**20c**. Interestingly, the results support that the order of the *Rf* values is nearly directly proportional to the Log P, that is, the hydrophobicity of **16a**, **c**—**20a**, **c**.

MIC Determination of Spacers C4 and C6 An assay of activity for bacteria, *E. coli* NIHJ JC-2 and *S. aureus* FDA 209P, was used to examine the difference in activity caused by the change in the configuration of the amino acid in double-stranded peptides, **17a**—**d** and **18a**—**d**. Bacteria were cultured for 24 h at 37 °C in 96-well micro plates.[11] Tables 4 and 5 show the minimum inhibitory concentration (MIC, μg/ml) for the growth of *E. coli* NIHJ JC-2 and *S. aureus* FDA 209P measured by treatment with the broth dilution method of double-stranded peptides. The MIC values show that these compounds were able to effectively inhibit the growth of *E. coli* NIHJ JC-2 and *S. aureus* FDA 209P. For the growth inhibition of *E. coli* NIHJ JC-2, compound **17b** is 16 times stronger than **17a**. In order to investigate the relationship between configuration patterns of the compounds and inhibitory activity, the antibacterial activity of compounds **18** was compared by a similar method. Similarly, the (D-, L-) isomer **18b** and (L-, D-) isomer **18c** were significantly more active than the (L-, L-) isomer **18a**, and the potency increases in the following order; (L-, L-) **18a**<(D-, D-) **18d**<(D-, L-) **18b**< and nearly equal to (L-, D-) **18c**. The antibacterial activities of compounds **17a**—**d** against *E. coli* NIHJ JC-2 and *S. aureus* FDA 209P also led to similar trends as shown in Fig. 3.

In the spacers with carbon numbers, n=4 and 6, the diastereomers **17c** and **18c** have a MIC of 16 and 8 μg/ml, respectively, while the enantiomers **17a**, **17d**, **18a**, and **18d** have MIC values in excess of about 200 μg/ml (Fig. 3b). Then, it is suggested that the antibacterial activity of double-stranded peptides is closely related with the difference in the mirror image and diastereomeric selective effects exist.

MIC Determination for Spacers C2 and C12 Our results also show a structure–activity relationship between anti-

Table 4. Comparative Biological Activities of Bis(AA_2–AA_1)-*N*,*N*-butane-1,4-diamine Analog *in Vitro*

Compound	Residues		*In vitro* MIC and MBC values (μg/ml)					
			E. coli NIHJ JC-2			*S. aureus* FDA 209P		
	AA_2	AA_1	MIC	MBC	$r^{a)}$	MIC	MBC	$r^{a)}$
17a	L-Phe	L-Phe	512	1024	2	128	256	2
17b	D-Phe	L-Phe	64	64	1	32	32	1
17c	L-Phe	D-Phe	64	64	1	16	16	1
17d	D-Phe	D-Phe	1024	1024	1	256	512	2

a) r=MBC/MIC.

Table 5. Comparative Biological Activities of Bis(AA_2–AA_1)-*N*,*N*-hexane-1,6-diamine Analog *in Vitro*

Compound	Residues		*In vitro* MIC and MBC values (μg/ml)					
			E. coli NIHJ JC-2			*S. aureus* FDA 209P		
	AA_2	AA_1	MIC	MBC	$r^{a)}$	MIC	MBC	$r^{b)}$
18a	L-Phe	L-Phe	1024	>1024	1	256	512	2
18b	D-Phe	L-Phe	32	64	2	8	16	2
18c	L-Phe	D-Phe	32	32	1	8	16	2
18d	D-Phe	D-Phe	512	>1024	2	256	1024	4

a) r=MBC/MIC.

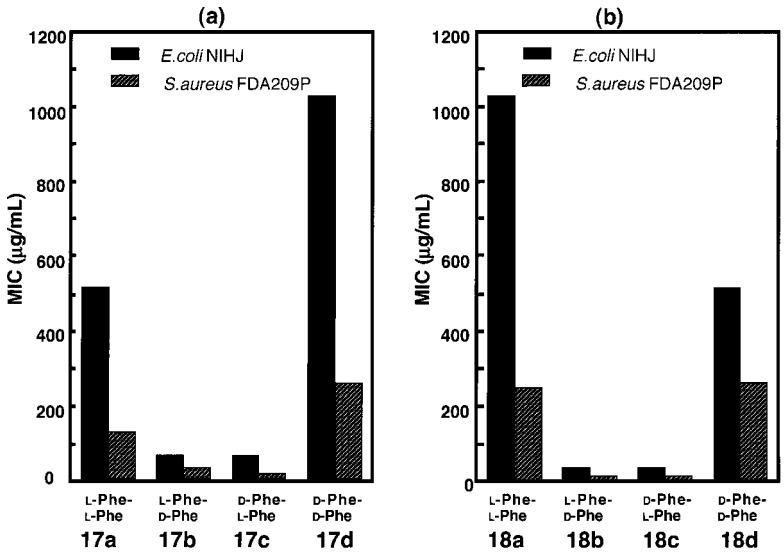

Fig. 3. Chirality Effect of Bis(y-Phe–x-Phe)-*N*,*N*-butane-1,4-diamines **17a**—**d** and Bis(y-Phe–x-Phe)-*N*,*N*-hexane-1,6-diamines **18a**—**d** on Activity against *E. coli* NIHJ JC-2 (a) and *S. aureus* FDA 209P (b)

Each bar show the mean of MIC.

bacterial activity and spacer length besides chirality. Here, we examined antibacterial activity for *E. coli* NIHJ JC-2 and *S. aureus* FDA 209P by stimulation of double-stranded peptides **16a**—**d** and **20a**—**d** which have a spacer length of C=2 and 12. In order to investigate the effect of the stereochemical configuration on bacterial proliferation, the activity against *E. coli* NIHJ JC-2 and *S. aureus* FDA 209P of four isomers of bis(y-Phe–x-Phe)-*N*,*N*-dodecane-1,12-diamine **20a**—**d** was tested. Figure 4 shows histograms of the data. Compound bis(L-Phe)-*N*,*N*-dodecane-1,12-diamine **10a** (carbon number=12) has 64 times the activity of **6a** (carbon number=2). It was interesting that the D-configuration, bis(D-Phe)-*N*,*N*-ethane-1,2-diamine **6b**, gave 4 times more activity than the L-configuration **6a** for anti-*S. aureus* FDA 209P proliferation. The antibacterial activity increases in the following order, (D-, D-) **20d**<(L-, L-) **20a**<(L-, D-) **20c**<(D-, L-) **20b**. The compound **20b** as diastereomers of **20a** and **20d** showed the most anti-*S. aureus* FDA 209P activity in this series, and has a MIC of 4 μg/ml. This trend is similar to the activity of **17a**—**d** and **18a**—**d** against the growth of *S. aureus* FDA 209P and *E. coli* NIHJ JC-2 (Fig. 4b). However, the four optical isomers **16a**—**d** were less active than **17**, **18**, and **20a**—**d**, and had a weaker chirality effect than **20a**—**d**.

Fluorescence Microscopy In order to examine the inter-

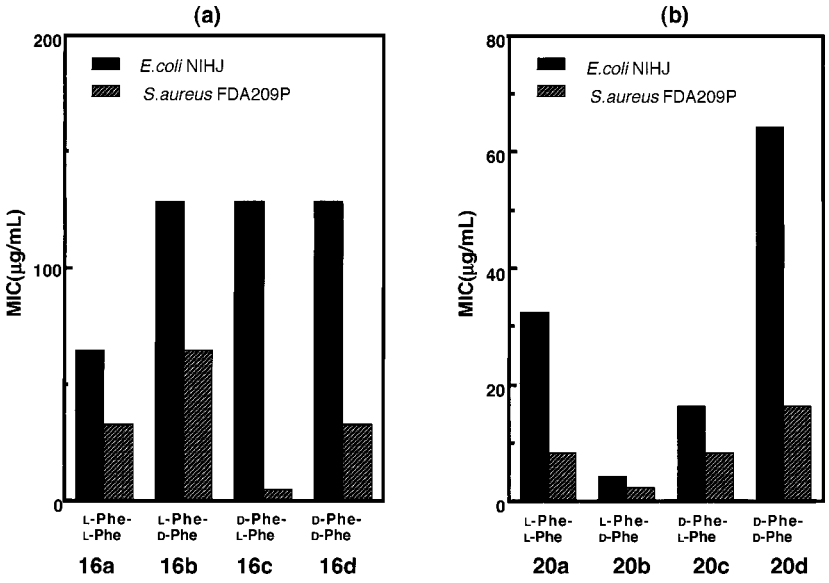

Fig. 4. Chirality Effect of Bis(y-Phe–x-Phe)-*N*,*N*-ethane-1,2-diamines **16a**—**d** and Bis(y-Phe–x-Phe)-*N*,*N*-dodecane-1,12-dimaines **20a**—**d** on Activity against *E. coli* NIHJ JC-2 (a) and *S. aureus* FDA 209P (b)

Each bar show the mean of MIC.

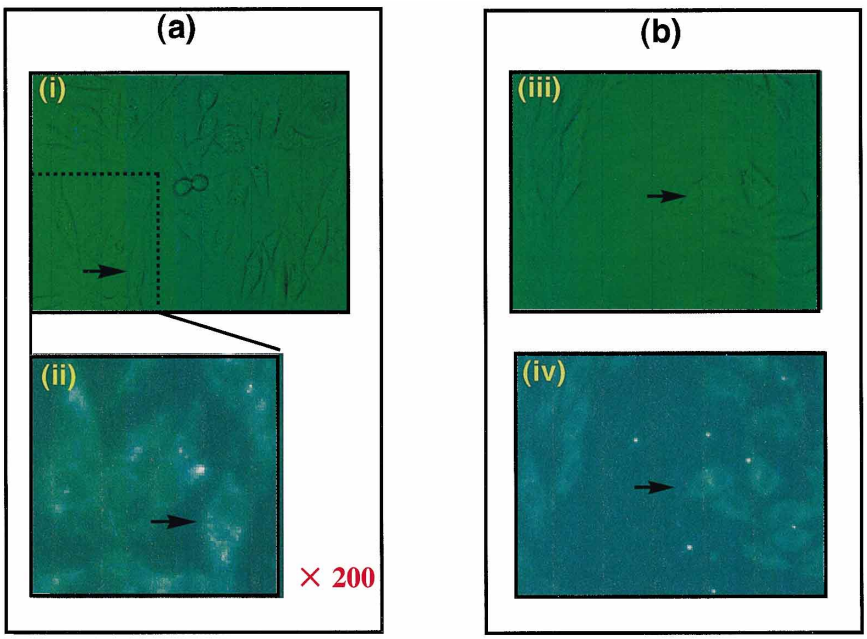

Fig. 5. Fluorescence Microscopic Images of A431 Cells after Treatment with New Fluorescent Labeling Bis(Dns–L-Phe)-*N*,*N*-ethane-1,2-diamine (**21**) Probe

A 431 cells were incubated with 27.5 μg/1000 μl (a) and 3.5 μg/1000 μl (b) of the fluorescent label **21** in DMEM containing 10% FBS at 37 °C for 24 h. λ_{ex}=349 nm, λ_{em}=530 nm, in 85% MeOH. Compound **21** was localized to the cell membrane and cytosol ((ii) and (iv)). Photographs (i) and (iii) without fluorescence are comparison of (ii) and (iv) with fluorescence. Magnification ×100 and ×200.

action between double-stranded peptide and cell membrane, the fluorescence probe bis(Dns–L-Phe)-*N*,*N*-ethane-1,2-diamine **21** conjugated to a known fluorescence reagent, dansyl (=Dns), to N-terminus of **6a** was synthesized. After 3×10^2 cells/ml of A431 cells seeded to 12-well plates were incubated for 48 h in a CO_2 incubater, 20 μl of each solution (27.5 μg/1000 μl and 3.5 μg/1000 μl) of fluorescence probe **21** was added and the mixture was incubated for 24 h. Figure 5 shows fluorescence photographs of A431 cells penetrated by **21** in the cytosol. Photographs (i), (ii) and (iii), (iv) correspond to compound **21** at 27.5 μg/1000 μl and 3.5 μg/1000 μl, respectively. A431 cells are stained at 3.5 μg/1000 μl. Moreover, photograph (iv) shows that compound **21** has a stained cytosol and membrane but not nucleus. The results imply that the double-stranded peptide, (L-Phe^2–L-Phe^1–)$_2$–spacer(S), also passes through the cell membrane, and is taken up into the cytosol.

Discussion

Peptides like gramicidines A and S, well known as anti-

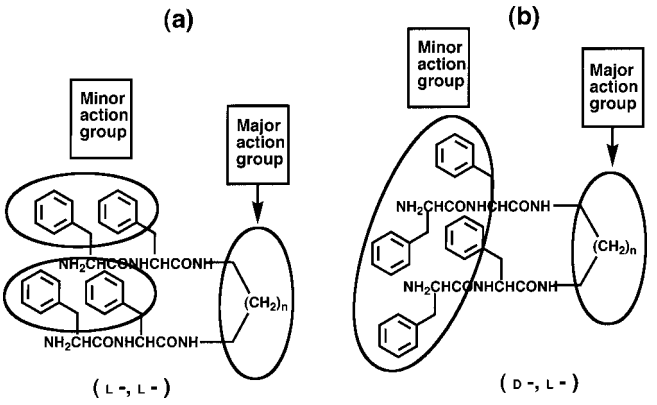

Fig. 6. Major and Minor Active Groups of (y-Phe–x-Phe)$_2$–Spacer Peptides for Diastereomeric Selective Antibacterial Activity

Symbols x and y show L- and D-configuration of Phe. Diastereomers (D-, L-) and (L-, D-) increase the growth inhibition for bacteria.

bacterial substances, are characterized by a wide antibacterial spectrum. It is suggested that gramicidine and other peptidal antibiotics act on the lipid matrix of the cell membrane, increase the membrane's permeability, and cause channels or pores to form.[12,13] However, the mechanism and structure–activity relationships of antibacterial peptides are still unknown. In this study, we demonstrated a structure–activity relationship between chirality and antibacterial activity based on values of MICs. In order to elucidate the effect of chirality on the antibacterial activity of artificial β-sheet-like double-stranded peptides, we examined the growth inhibition of *E. coli* and *S. aureus*. The effect, particularly on diastereomeric selective activity, was found in the MICs of four optical isomers, **17a**—**d**, **18a**—**d**, and **20a**—**d**, conjugated –y-Phe–x-Phe– sequences to the two N-terminals of the spacer. In the series of bis(y-Phe–x-Phe)-*N*,*N*-hexane-1,6-diamine **18a**—**d**, for instance, the antibacterial activity for gram-negative *E. coli* NIHJ JC-2 increase of within 32 from 1024 μg/ml in the following order: (L-, L-)<(D-, D-)<(L-, D-)~(D-, L-). For gram-positive *S. aureus* FDA 209P proliferation, although the order of antibacterial activity was similar, the activity of compounds **18a**—**d** was greater to gram-positive bacteria than to gram-negative one. It is concluded that the potency of the (L-, D-) and (D-, L-) forms are stronger than that of (L-, L-) and (D-, D-) forms. Then, the diastereomeric (D-, L-) and (L-, D-) forms for the (L-, L-) form, interestingly, may be the best antibacterial configuration (=bioactive structure).

The molecular size of the spacer also may relate to antibacterial activity since our data support that bis(x-Phe)-*N*,*N*-dodecane-1,12-diamine and bis(y-Phe–x-Phe)-*N*,*N*-dodecane-1,12-diamine are more active than bis(x-Phe)-*N*,*N*-ethane-1,2-diamine and bis(y-Phe–x-Phe)-*N*,*N*-ethane-1,2-diamine. The analog **18a** is less active than **16a**. The activity of double-stranded peptides increases in the following order: C(6)<C(8)<C(4)<C(2)<C(12) (the number shows the number of carbons in the spacer). These results suggest that the spacer length and chirality are related to the activity of double-stranded peptides against *E. coli* and *S. aureus*. Changing the chirality and spacer length, therefore, is important to the design of more active double-stranded peptides. The results suggest that there are two action groups in double-stranded peptides: first, spacer length, and second, the chirality of the side chain of the phenylalanine residue, as shown in Fig. 6.

The membrane and cell wall are located on the bacterial envelope, and the chemicals, hormones, and small proteins pass through porin to the inner cell. The double-stranded peptides are more active against *S. aureus* (gram-positive bacteria) than *E. coli* (gram-negative bacteria) which have porins located in the membrane. In gram-negative bacteria, *E. coli*, the most active bis(L-Phe–D-Phe)-*N*,*N*-dodecane-1,12-diamine **20c** would be taken up into the cytosol through porin, which suggests antibacterial activity. The data suggests that the passage of porin is not always related to the antibacterial activity. When the double-stranded peptide is taken up into the cytosol, the structure is changed. As antibacterial peptides generally form a peptide-lipid complex pore, a fluorescence probe **21** conjugated to the dansyl group of **6a** was synthesized to examine which of the double-stranded peptides passes through the membrane. Figure 5 shows fluorescence photographs of A431 cells treated with **21**. It shows that compound **21** entered the cytosol, but not the nucleus. It suggests, therefore, that double-stranded peptides also would be taken up by the cytosol or form double-stranded peptides channels (or pores) on the memberane, and express antibacterial activity. Recent our investigations showed that the –D-Phe–L-Phe– sequence increases the membrane permeability of Ca^{2+} ion by Fura-2[14] analysis as compared with the –D-Phe–L-Phe– sequence. This evidence supports that compounds **18b** and **20b**, *etc*. form channels or pores *via* double-stranded peptides.

Replacement of the –L-Phe–L-Phe– by –D-Phe–L-Phe– (or –L-Phe–D-Phe–) sequence in compounds **1** led to a more active antibacterial effect. From these results, the diastereomeric selective antibacterial activities clearly indicate that the membrane permeability is linked to the chiral plane of **17b**, **c**, **18b**, **c**, and **20b**, **c**, *etc.* Because, the *Rf* value of **18c** conjugated –D-Phe–L-Phe– (or –L-Phe–D-Phe–) is smaller than that of **18a** conjugated –L-Phe–L-Phe– as listed in Table 1. The *Rf* values represent the polarity of compounds, *i.e*. **18c** has higher polarity than **18a**. When high log P and polar diastereomers, **16b**—**c**, **17b**—**c**, **18b**—**c**, and **20b**—**c**, *etc.* pass through the cell membrane, it is suggested that the polarity of the membrane increases. At present, we can not explain the order of potency of double-stranded peptides against, *E. coli* and *S. aureus*.

Conclusions

In this paper, we described the characterization and conformation of mini parallel double-stranded peptides and demonstrated a structure–activity relationship for micro bacterial growth inhibition. Here our study showed that the (D-, L-) or (L-, D-) forms are the most active configurations in bis(y-Phe–x-Phe)-*N*,*N*-ethane-1,2-diamine, -*N*,*N*-butane-1,4-diamine, -*N*,*N*-hexane-1,6-diamine, and -*N*,*N*-dodecane-1,12-diamine. This suggests that the configurations, (D-, L-) or (L-, D-), are probably bio-active conformations in double-stranded peptides (L-Phe^2–L-Phe^1)$_2$–spacer(S). Measured differences of the activity show the highly stereospecific pharmacokinetic phenomena of the double-stranded peptides for *E. coli* or *S. aureus* and may relate to the penetration or pore forming ability of mini double-stranded peptides in the microbacterial membrane. We are interested in designing and synthesizing better anti-methicillin-resistant *Staphylococcus*

aureus (MRSA) drugs by changing the chirality and spacer length. Clinical bed sides are exposed to the menace of MRSA, and the molecular design and synthesis of anti-MRSA drugs are expected in the field of chemotherapy. In antibacterial peptidal drug design, our results show that specified chirality, (D-, L-) or (L-, D-), in double-stranded peptides plays an important role in anti-bacterial activity. Further studies are in progress to elucidate the diastereomeric selective effects on growth inhibition of several cells.

Experimental

Melting points were taken on a Yanako (MP-21) apparatus and are uncorrected. IR spectra were recorded with a JASCO A-100 spectrophotometer and UV–visible spectra with a JASCO U-best 30 spectrophotometer. ^{1}H- and ^{13}C-NMR spectra were recorded with a JNM GX-270 (270 MHz) or α-500 (500 MHz) spectrometer with TMS (tetramethyl silane) as an internal standard. FAB mass spectral data were recorded with a JEOL JMS-HX110 spectrometer, and relevant data are tabulated as *m/z*. TLC was performed using Silica gel 60 F254 (Merck) plates and the following solvent systems: $CHCl_3$–MeOH (20 : 1) (A) and $CHCl_3$–MeOH (10 : 1) (B). The peptides were detected on the TLC plates using iodine vapor or UV absorption. Silica gel column chromatography was performed on Wako gel C-200 (100 mesh) or Merck Silica gel 60N (100 mesh). Analytical reverse phase HPLC was carried out on a TOSO CCPD system equipped with a Tskgel (ODS-120T) column. Elemental analyses were performed by the Laboratory Center of Elemental Analysis, University of Ehime (Japan). For all UV–vis and CD spectra, commercial solvents of the highest purity available were used.

Synthesis A series of double-stranded peptides were synthesized as described in our previous paper. New compounds **2**—**4**, **7**—**9**, **12**—**14**, and **17**—**19** were prepared from the corresponding protected peptide analogs by a reaction with protected amino acids of the spacer according to previously published procedures.[7)]

The General Procedure for the Synthesis of Bis(Boc–L-Phe)-*N*,*N*-butane-1,4-diamine (2a) *tert*-Butoxycarbonyl phenylalanine (Boc–L-PheOH) (3.20 g, 12.1 mmol) and CDI (2.20 g, 13.5 mmol) were dissolved in dry $CHCl_3$ and were stirred at room temperature for 1 h. To this a solution 1,4-diaminobutane (0.48 g, 5.5 mmol) was added, and the resulting mixture was stirred overnight, and the solvent was evaporated. After the addition of cooled aq. MeOH, the solid was collected, and washed with aq. MeOH, 5% citric acid, 5% sodium hydrogen carbonate and water, and dried *in vacuo*. Further purification by silicagel column chromatography (eluted with stepwise: $CHCl_3$ and 2% MeOH/$CHCl_3$) gave the product **2a** as a colorless crystal in 75% yield: *Rf* (A) 0.463; mp 197 °C; FAB-MS (NBA=nitrobenzyl alcohol) *m/z* 583 $(M+H)^+$. *Anal.* Calcd for $C_{32}H_{46}N_4O_6$ C, 65.96; H, 7.96; N, 9.61. Found: C, 65.83; H, 7.88; N, 9.38.

The Other Boc Double-Stranded Peptides Bis(Boc–D-Phe)-*N*,*N*-butane-1,4-diamine **2b**: 78% yield: *Rf* (A) 0.463; mp 197—198 °C; FAB-MS (NBA) *m/z* 583 $(M+H)^+$. Bis(Boc–L-Phe–L-Phe)-*N*,*N*-butane-1,4-diamine **12a**: 70% yield: *Rf* (A) 0.337; mp 222—224 °C; *Anal.* Calcd for $C_{50}H_{64}N_6O_8 \cdot 1/2H_2O$: C, 67.77; H, 7.39; N, 9.48. Found: C, 67.87; H. 7.29: N, 9.55. Bis(Boc–D-Phe–L-Phe)-*N*,*N*-butane-1,4-diamine **12b**: *Rf* (A) 0.395; mp 213—214 °C; HR-FAB-MS (NBA) Found 877.4868, Calcd for $C_{50}H_{64}N_6O_8$ 877.4864 $(M+H)^+$. Bis(Boc–L-Phe–D-Phe)-*N*,*N*-butane-1,4-diamine **12c**: *Rf* (A) 0.395; mp 215—217 °C; HR-FAB-MS (NBA) Found 877.4882, Calcd for $C_{50}H_{64}N_6O_8$ 877.4864 $(M+H)^+$. Bis(Boc–D-Phe–D-Phe)-*N*,*N*-butane-1,4-diamine **12d**: *Rf* (A) 0.337; mp 200—201 °C (aq. MeOH); FAB-MS (NBA) *m/z* 877 $(M+H)^+$. Bis(Boc–L-Phe)-*N*,*N*-hexane-1,6-diamine **3a**: *Rf* (A) 0.585; mp 171—172 °C; FAB-MS (NBA) *m/z* 611 $(M+H)^+$. Bis(Boc–D-Phe)-*N*,*N*-hexane-1,6-diamine **3b**: 85% yield: *Rf* (A) 0.58; mp 172—173 °C; FAB-MS (NBA) *m/z* 611 $(M+H)^+$. Bis(Boc–L-Phe–L-Phe)-*N*,*N*-hexane-1,6-diamine **13a**: *Rf* (A) 0.386; mp 210—212 °C; FAB-MS (NBA) *m/z* 905 $(M+H)^+$. Bis(Boc–D-Phe–L-Phe)-*N*,*N*-hexane-1,6-diamine **13b**: 87% yield; *Rf* (A) 0.390; mp 214—215 °C; FAB-MS (NBA) *m/z* 905 $(M+H)^+$. Bis(Boc–L-Phe–D-Phe)-*N*,*N*-hexane-1,6-diamine **13c**: 80% yield; *Rf* (A) 0.390; mp 216—217 °C; HR-FAB-MS (NBA) Found 905.5156, Calcd for $C_{52}H_{68}N_6O_8$ 905.5177. Bis(Boc–D-Phe–D-Phe)-*N*,*N*-hexane-1,6-diamine **13d**: 72% yield; *Rf* (A) 0.386; mp 211—213 °C; HR-FAB-MS (NBA) Found 705.4133, Calcd for $C_{52}H_{68}N_6O_8$ 705.4128 $(M+H)^+$. Bis(Boc–L-Phe)-*N*,*N*-octane-1,8-diamine **4a**: 71% yield: *Rf* (A) 0.654; mp 175—178 °C; FAB-MS (NBA) *m/z* 639 $(M+H)^+$. Bis(Boc–D-Phe)-*N*,*N*-octane-1,8-diamine **4b**: 75% yield: *Rf* (A) 0.654; mp 174—177 °C. Bis(Boc–L-Phe–L-Phe)-*N*,*N*-octane-1,8-diamine **14a**: 85% yield: *Rf* (A) 0.384; mp 159—162 °C; FAB-MS (NBA) *m/z* 933 $(M+H)^+$. Bis(*Z*-L-Phe–D-Phe)-*N*,*N*-octane-1,8-diamine **14c**: 85% yield: *Rf* (A) 0.423; mp 197—199 °C. FAB-MS (NBA) *m/z* 933 $(M+H)^+$. Bis(Boc–D-Phe–D-Phe)-*N*,*N*-octane-1,8-diamine **14d**: 68% yield: *Rf* (A) 0.384; mp 157—160 °C; FAB-MS (NBA) *m/z* 933 $(M+H)^+$. *Anal.* Calcd for $C_{42}H_{52}N_6O_4 \cdot 1/2H_2O$: C, 68.84; H, 7.81; N, 8.92. Found: C, 68.90; H, 7.84; N, 9.11.

The General Procedure for the Synthesis of Bis(L-Phe)-*N*,*N*-butane-1,4-diamine (7a) A mixture of 1.00 g (1.14 mmol) of **2a** and 10 ml of TFA was stirred for 1 h in an ice bath. After a 1 M NaOH/5% $NaHCO_3$ workup, the solution was extracted with $CHCl_3$. The organic layers were combined, dried over Na_2SO_4, filtrated, concentrated under vacuum, and dried to give colorless crystals of **7a**: 81.0% yield, and the product was purified by column chromatography on silica gel (35.0 g) eluted with $CHCl_3$ and 3% MeOH/$CHCl_3$ (stepwise elution): *Rf* (A) 0.056, mp 126—128 °C (from ether/$CHCl_3$). ^{1}H-NMR (signal assignments from the spectra of H–H and H–C COSYs at 500 MHz, $CDCl_3$/DMSO-d_6 (0.5 ml/0.2 ml)) δ: 1.35—1.38 (m, 4H, –C<u>H</u>$_2$–×2), 2.66 (dd, 2H, *J*=8.2, 13.4 Hz, Phe–C<u>H</u>–×2), 3.01 (dd, 2H, *J*=4.9, 13.4 Hz, Phe–C<u>H</u>–×2), 3.10 (m, 4H, –C<u>H</u>$_2$–NHCO–×2), 3.44 (dd, 2H, *J*=4.9, 8.2 Hz, –C$^{\alpha}$<u>H</u>–×2), 7.17—7.28 (m, 10H, Ar-H×2), and 7.72 (t, 2H, *J*=5.6 Hz, –N<u>H</u>CO–×2). ^{13}C-NMR (signal assignments from the spectra of C–H COSY at 500 Mz, $CDCl_3$/DMSO-d_6 (0.5 ml/0.2 ml)) ppm 26.53 (C^2), 38.18 (C^1), 41.24 (Phe–<u>C</u>H–), 56.32 (–C$^{\alpha}$–), 126.12 (*p*-), 128.09 (*m*-), 129.18 (*o*-), 138.43 (φ-), and 174.13 (–NHCO–). IR (KBr) cm^{-1}; 3270 and 1640. FAB-MS (NBA) *m/z* 383 $(M+H)^+$.

Bis(L-Phe)-*N*,*N*-butane-1,4-diamine **7b**: *Rf* (A) 0.056; mp 126—127 °C. FAB-MS (NBA) *m/z* 383 $(M+H)^+$.

Bis(L-Phe–L-Phe)-*N*,*N*-butane-1,4-diamine (17a) 70% yield, *Rf* (B) 0.41: mp 161—162 °C (from ether/$CHCl_3$). ^{1}H-NMR (signal assignments from the spectra of H–H COSY at 500 MHz, $CDCl_3$/DMSO-d_6 (0.5 ml/0.2 ml)) δ: 1.33—1.36 (m, 4H, –CH_2–×2), 2.48 (dd, 2H, *J*=8.85, 13.7 Hz, Phe^2–C<u>H</u>–×2), 2.92 (dd, 2H, *J*=7.6, 13.7 Hz, Phe^1–C<u>H</u>–×2), 2.97 (dd, 2H, *J*=4.3, 13.7 Hz, Phe^2–C<u>H</u>–×2), 3.03 (dd, 2H, *J*=6.1, 13.8 Hz, Phe^1–C<u>H</u>–×2), 3.08 (m, 2H, –C<u>H</u>$_2$–NHCO–×2), 3.50 (dd, 2H, *J*=4.3, 8.85 Hz, –C$^{\alpha 2}$H–×2), 4.63 (ddd, 2H, *J*=6.1, 7.6, 8.5 Hz, –C$^{\alpha 1}$H–×2), 7.12—7.28 (m, 5H, Ar-H), 7.58 (t, 2H, *J*=5.5 Hz, –NH^{a}CO–×2), and 7.94 (d, 2H, *J*=8.5 Hz, –NH^{b}CO–×2). ^{13}C-NMR (signal assignments from the spectra of C–H COSY at 500 Mz, $CDCl_3$/DMSO-d_6 (0.5ml/0.2 ml)) ppm 26.32 (C^2), 38.34 (Phe–<u>C</u>H–, –<u>C</u>H$_2$–NH–), 40.59 (Phe–<u>C</u>H–), 53.34 (–C$^{\alpha 1}$–), 56.09 (–C$^{\alpha 2}$–), 126.13 (p^1-), 126.21 (p^2-), 127.91 (o^1-), 128.58 (o^2-), 129.17 (m^1-), 129.23 (m^2-), 137.33 (φ^1-), 138.27 (φ^2-), 170.54 (–NH^{b}CO–), and 173.77 (–NH^{a}CO–). IR (KBr) cm^{-1}; 3270 and 1640. *Anal.* Calcd for $C_{40}H_{48}N_6O_4 \cdot 1/2H_2O$: C, 70.05 H, 7.20; N, 12.25. Found: C, 70.17; H. 7.11: N, 12.28.

Bis(D-Phe–L-Phe)-*N*,*N*-butane-1,4-diamine (17b) Compound **17b** was prepared in a similar manner to **7a** and obtained as a colorless solid in 86% yield: *Rf* (B) 0.16, mp 192—194 °C (from ether/$CHCl_3$). ^{1}H-NMR (signal assignments from the spectra of H–H COSY at 500 MHz, $CDCl_3$/DMSO-d_6 (0.5 ml/0.2 ml)) δ: 1.32—1.36 (m, 4H, –CH_2–×2), 2.57 (m, 2H, Phe^2–CH–×2), 2.91 (dd, 2H, *J*=7.9, 13.7 Hz, Phe^1–CH–×2), 3.01 (m, 2H, Phe^2–CH–×2), 3.03 (dd, 2H, *J*=6.1, 13.7 Hz, Phe^1–CH–×2), 3.08—3.09 (m, 4H, –C<u>H</u>$_2$–NHCO–×2), 3.49 (dd, 2H, *J*=4.6, 8.2 Hz, –C$^{\alpha 2}$H–×2), 4.6 (ddd, 1H, *J*=6.4, 7.9, 8.2 Hz, –C$^{\alpha 1}$H–×2), 7.15—7.19 (m, 12H, *o*-, *p*-), 7.20—7.26 (m, 8H, *m*-), 7.56 (t, 2H, *J*=5.5 Hz, –NH^{a}CO–×2), and 8.01 (d, 2H, *J*=8.2 Hz, –NH^{b}CO–×2). ^{13}C-NMR (signal assignments from the spectra of C–H COSY at 500 Mz, $CDCl_3$/DMSO-d_6 (0.5 ml/0.2 ml)) ppm 26.27 (C^2), 38.23 (Phe^1–<u>C</u>H–), 38.58 (–<u>C</u>H$_2$–NH–), 40.93 (Phe^2–<u>C</u>H–), 53.99 (–<u>C</u>$^{\alpha 1}$–), 56.20 (–<u>C</u>$^{\alpha 2}$–), 126.33 (p^1-), 126.39 (p^2-), 128.09 (m^1-), 128.26 (m^2-), 129.18 (o^1-), 129.22 (o^2-), 137.29 (φ^1-), 138.06 (φ^2-), 170.86 (–NH^{b}CO–), and 173.89 (–NH^{a}CO–). IR (KBr) cm^{-1}; 3270 and 1640, FAB-MS (NBA) *m/z* 677 $(M+H)^+$.

Bis(L-Phe–D-Phe)-*N*,*N*-butane-1,4-diamine (17c) Compound **17c** was prepared in a similar manner to **17a** and obtained as a colorless solid in 78% yield: *Rf* (B) 0.16; mp 190—193 °C; FAB-MS (NBA) *m/z* 677 $(M+H)^+$.

Bis(D-Phe–D-Phe)-*N*,*N*-butane-1,4-diamine (17d) Compound **17d** was prepared in a similar manner to **17a** and obtained as a colorless solid in 70% yield: *Rf* (B) 0.41, mp 160—163 °C; FAB-MS (NBA) *m/z* 677 $(M+H)^+$.

Bis(L-Phe)-*N*,*N*-hexane-1,6-diamine (8a) Compound **8a** was prepared in a similar manner to **3a** and obtained as a colorless solid in 65% yield: *Rf* (B) 0.108, mp 122—123 °C (from ether/$CHCl_3$). ^{1}H-NMR (signal assignments from the spectra of H–H and H–C COSYs at 500 MHz, $CDCl_3$/DMSO-d_6 (0.5 ml/0.2 ml)) δ: 1.275—1.289 (m, 2H, –C<u>H</u>$_2$–), 1.452—1.479 (m, 2H, –C<u>H</u>$_2$–), 2.72 (dd, 1H, *J*=8.85, 13.7 Hz, Phe–C<u>H</u>–), 3.17 (dd, 1H, *J*=4.6, 13.7 Hz, Phe–C<u>H</u>–), 3.20 (m, 2H, –C<u>H</u>$_2$–NHCO–), 3.57 (dd, 1H, *J*=4.6, 8.85 Hz, –C$^{\alpha}$<u>H</u>–), 7.21—7.31 (m, 5H, Ar-H), and 7.48 (m, 1H,

–NHCO–). ^{13}C-NMR (signal assignments from the spectra of C–H COSY at 500 Mz, $CDCl_3$/DMSO-d_6 (0.5 ml/0.2 ml)) ppm 26.25 (C^3), 29.26 (C^2), 38.69 (C^1), 41.04 (Phe–CH–), 56.35 (–C^{α}–), 126.53 (*p*-), 128.44 (*m*-), 129.28 (*o*-), 138.02 (φ-), and 174.05 (–NHCO–). IR (KBr) cm^{-1}; 3270 and 1640; FAB-MS (NBA) *m/z* 411 (M+H)$^+$. *Anal.* Calcd for $C_{24}H_{34}N_4O_2$: C, 70.21; H, 8.35; N, 13.65. Found: C, 70.03; H, 8.26; N, 13.57.

Bis(D-Phe)-*N*,*N*-hexane-1,6-diamine (8b) Compound **8b** was prepared in a similar manner to **8a** and obtained as a colorless solid in 80% yield: *Rf* (B) 0.108; mp 121—122.5 °C; FAB-MS (NBA) *m/z* 411 (M+H)$^+$.

Bis(L-Phe–L-Phe)-*N*,*N*-hexane-1,6-diamine (18a) Compound **18a** was prepared in a similar manner to **3a** and obtained as a colorless solid in 72% yield: *Rf* (B) 0.42, mp 190—191 °C (from ether/MeOH). ^{1}H-NMR (signal assignments from the spectra of H–H COSY at 500 MHz, $CDCl_3$/DMSO-d_6 (0.5 ml/0.2 ml)) δ: 1.19—1.23 (m, 4H, –CH$_2$–×2), 1.34—1.40 (m, 4H, –CH$_2$–×2), 2.49 (dd, 2H, *J*=8.85, 13.7 Hz, Phe^2–CH–×2), 2.93 (dd, 2H, *J*=7.6, 13.0 Hz, Phe^1–CH–×2), 2.98 (dd, 2H, *J*=4.5, 14.0 Hz, Phe^2–CH–×2), 3.03 (dd, 2H, *J*=6.0, 14.0 Hz, Phe^1–CH–×2), 3.04—3.11 (m, 4H, –CH$_2$–NHCO–×2), 3.51 (dd, 2H, *J*=4.5, 8.85 Hz, –C$^{\alpha 2}$H–×2), 4.64 (ddd, 2H, *J*=6.0, 7.6, 8.85 Hz, –C$^{\alpha 1}$H–×2), 7.14—7.17 (m, 8H, 2H×4, *o*-), 7.18—7.28 (m, 12H, 3H×4, *m*-, *p*-), 7.53 (t, 2H, *J*=5.8 Hz, –NH^{a}CO–×2), and 7.95 (d, 2H, *J*=8.85 Hz, –NH^{b}CO–×2). ^{13}C-NMR (signal assignments from the spectra of C–H COSY at 500 Mz, $CDCl_3$/DMSO-d_6 (0.5 ml/0.2 ml)) ppm 25.79 (C^3), 28.97 (C^2), 38.37 (Phe^1–C$^{\beta}$–), 38.71 (C^1), 42.67 (Phe^2–C$^{\beta}$–), 53.81 (Phe^1–C$^{\alpha}$–), 56.17 (Phe^2–C$^{\alpha}$–), 126.52 (p^1-), 126.58 (p^2-), 128.17 (m^1-), 128.45 (m^2-), 129.20 (o^1-), 129.33 (o^2-), 137.12 (φ^1-), 137.68 (φ^2-), 170.82 (–NH^{b}CO–), and 173.79 (–NH^{a}CO–). IR (KBr) cm^{-1}; 3270 and 1640. *Anal.* Calcd for $C_{42}H_{52}N_6O_4\cdot 1/2H_2O$: C, 70.66; H, 7.48; N, 11.77. Found: C, 71.19; H. 7.37; N, 11.78.

Bis(D-Phe–L-Phe)-*N*,*N*-hexane-1,6-diamine (18b) Compound **18b** was prepared in a similar manner to **18a** and obtained as a colorless solid in 68% yield: *Rf* (B) 0.21, mp 161—162 °C (from ether/MeOH). ^{1}H-NMR (signal assignments from the spectra of H–H COSY at 500 MHz, $CDCl_3$/DMSO-d_6 (0.5 ml/0.2 ml)) δ: 1.18—1.21 (m, 4H, –CH$_2$–×2), 1.35—1.41 (m, 4H, –CH$_2$–×2), 2.58 (dd, 2H, *J*=8.85, 13.4 Hz, Phe^2–CH–×2), 2.92 (dd, 2H, *J*=7.9, 13.7 Hz, Phe^1–CH–×2), 3.03 (dd, 2H, *J*=6.4, 13.7 Hz, Phe^1–CH–×2), 3.05 (dd, 2H, *J*=4.6, 13.4 Hz, Phe^2–CH–×2), 3.08—3.14 (m, 4H, –CH$_2$–NHCO–×2), 3.50 (dd, 2H, *J*=4.6, 8.85 Hz, –C$^{\alpha 2}$H–×2), 4.64 (ddd, 2H, *J*=6.4, 7.9, 8.5 Hz, –C$^{\alpha 1}$H–×2), 7.14—7.24 (m, 20H, 10H×2), 7.52 (t, 2H, *J*=5.5 Hz, –NH^{a}CO–×2), and 8.00 (d, 2H, *J*=8.5 Hz, –NH^{b}CO–×2). ^{13}C-NMR (signal assignments from the spectra of C–H COSY at 500 Mz, $CDCl_3$/DMSO-d_6 (0.5 ml/0.2 ml)) ppm 25.90 (C^3), 28.95 (C^2), 38.32 (Phe^1–C$^{\beta}$–), 38.67 (C^1), 40.88 (Phe^2–C$^{\beta}$–), 53.98 (Phe^1–C$^{\alpha}$–), 56.16 (Phe^2–C$^{\alpha}$–), 126.32 (p^1-), 126.38 (p^2-), 128.06 (m^1-), 128.25 (m^2-), 129.17 (o^1-), 129.24 (o^2-), 137.28 (φ^1-), 138.04 (φ^2-), 170.82 (–NH^{b}CO–), and 173.86 (–NH^{a}CO–). IR (KBr) cm^{-1}; 3270 and 1640. *Anal.* Calcd for $C_{42}H_{52}N_6O_4\cdot 1/2H_2O$: C, 70.66; H, 7.48; N, 11.77. Found: C, 71.08; H, 7.38; N, 11.77.

Bis(L-Phe–D-Phe)-*N*,*N*-hexane-1,6-diamine (18c) Compound **18c** was prepared in a similar manner to **18a** and obtained as a colorless solid in 70% yield: *Rf* (B) 0.21, mp 160—161 °C (from ether/MeOH). ^{1}H-NMR (signal assignments from the spectra of H–H COSY at 500 MHz, $CDCl_3$/DMSO-d_6 (0.5 ml/0.2 ml)) δ: 1.18—1.23 (m, 4H, –CH$_2$–×2), 1.36—1.39 (m, 4H, –CH$_2$–×2), 2.57 (dd, 2H, *J*=8.5, 13.4 Hz, Phe^2–CH–×2), 2.92 (dd, 2H, *J*=7.6, 13.4 Hz, Phe^1–CH–×2), 3.00 (dd, 2H, *J*=4.27, 13.4 Hz, Phe^2–CH–×2), 3.03 (dd, 2H, *J*=6.4, 13.4 Hz, Phe^1–CH–×2), 3.05—3.15 (m, 4H, –CH$_2$–NHCO–×2), 3.49 (dd, 2H, *J*=4.27, 8.5 Hz, –C$^{\alpha 2}$H–×2), 4.63 (ddd, 2H, *J*=6.4, 7.6, 8.5 Hz, –C$^{\alpha 1}$H–×2), 7.11—7.14 (m, 8H, 2H×4, *o*-), 7.16—7.26 (m, 12H, 3H×4, *m*-, *p*-), 7.52 (t, 2H, *J*=5.5 Hz, –NH^{a}CO–×2), and 8.00 (d, 2H, *J*=8.5 Hz, –NH^{b}CO–×2). ^{13}C-NMR (signal assignments from the spectra of C–H COSY at 500 Mz, $CDCl_3$/DMSO-d_6 (0.5 ml/0.2 ml)) ppm 25.88 (C^3), 28.95 (C^2), 38.32 (Phe^1–C$^{\beta}$–), 38.67 (C^1), 40.84 (Phe^2–C$^{\beta}$–), 54.01 (Phe^1–C$^{\alpha}$–), 56.15 (Phe^2–C$^{\alpha}$–), 126.36 (p^1-), 126.40 (p^2-), 128.08 (m^1-), 128.28 (m^2-), 129.17 (o^1-), 129.24 (o^2-), 137.27 (φ^1-), 137.98 (φ^2-), 170.80 (–NH^{b}CO–), and 173.82 (–NH^{a}CO–). IR (KBr) cm^{-1}; 3270 and 1640; FAB-MS (NBA) *m/z* 705 (M+H)$^+$.

Bis(D-Phe–D-Phe)-*N*,*N*-hexane-1,6-diamine (18d) Compound **3b** was prepared in a similar manner to **3a** and obtained as a colorless solid in 75% yield: *Rf* (B) 0.42, mp 193—194 °C; FAB-MS (NBA) *m/z* 705 (M+H)$^+$.

Bis(L-Phe)-*N*,*N*-octane-1,8-diamine (9a) Compound **9a** was prepared in a similar manner to **3a** and obtained as a colorless solid in 75% yield: *Rf* (B) 0.16; mp 105—106.5 °C (from ether/$CHCl_3$). ^{1}H-NMR (signal assignments from the spectra of H–H and H–C COSYs at 500 MHz, $CDCl_3$) δ: 1.28—1.31 (m, 8H, –CH$_2$–CH$_2$–×2), 1.45—1.50 (m, 4H, –CH$_2$–×2), 2.69 (dd, 2H, *J*=9.2, 13.7 Hz, Phe–CH–×2), 3.21—3.24 (m, 4H, –CH$_2$–NHCO–×2), 3.27 (dd, 2H, *J*=3.96, 13.7 Hz, Phe–CH–×2), 3.59 (dd, 2H, *J*=3.96, 9.2 Hz, –C$^{\alpha}$H–×2), 7.21—7.33 (m, 12H, 5H×2, –NHCO–×2). ^{13}C-NMR (signal assignments from the spectra of C–H COSY at 500 Mz, $CDCl_3$/DMSO-d_6 (0.5 ml/0.2 ml)) ppm 26.58 (C^4), 28,90 (C^3), 29.26 (C^2), 38.76 (C^1), 41.06 (Phe–CH–), 56.27 (–C^{α}–), 126.34 (*p*-), 128.77 (*m*-), 129.20 (*o*-), 138.02 (φ-), and 173.97 (–NHCO–). IR (KBr) cm^{-1}; 3270 and 1640.

Bis(D-Phe)-*N*,*N*-octane-1,8-diamine (9b) Compound **3b** was prepared in a similar manner to **3a** and obtained as a colorless solid in 70% yield: *Rf* (B) 0.16, mp 104—106 °C; FAB-MS (NBA) *m/z* 439 (M+H)$^+$.

Bis(L-Phe–L-Phe)-*N*,*N*-octane-1,8-diamine (19a) Compound **19a** was prepared in a similar manner to **3a** and obtained as a colorless solid in 70% yield: *Rf* (A) 0.43, mp 170—172 °C (from ether/$CHCl_3$). ^{1}H-NMR (signal assignments from the spectra of H–H COSY at 500 MHz, $CDCl_3$/DMSO-d_6 (0.5 ml/0.2 ml)) δ: 1.14—1.23 (m, 8H, –CH$_2$–CH$_2$–×2), 1.34—1.41 (m, 4H, –CH$_2$–×2), 2.53 (dd, 2H, *J*=8.85, 13.4 Hz, Phe^2–CH–×2), 2.92 (dd, 2H, *J*=7.6, 13.7 Hz, Phe^1–CH–×2), 2.98 (dd, 2H, *J*=4.3, 13.4 Hz, Phe^2–CH–×2), 3.03 (dd, 2H, *J*=7.6, 13.7 Hz, Phe^1–CH–×2), 3.06—3.11 (m, 4H, –CH$_2$–NHCO–×2), 3.51 (dd, 2H, *J*=4.3, 8.85 Hz, Phe^2–C$^{\alpha 2}$H–×2), 4.63 (ddd, 2H, *J*=7.3, 7.6, 8.85 Hz, Phe^1–C$^{\alpha 1}$H–×2), 7.13—7.19 (m, 8H, o^1-, o^2-, 4H×2), 7.21—7.26 (m, 12H, *m*-, *p*-, 6H×2), 7.54 (t, 2H, *J*=5.5 Hz, –NH^{a}CO–×2), 7.95 (d, 2H, *J*=8.85 Hz, –NH^{b}CO–×2). ^{13}C-NMR (signal assignments from the spectra of C–H COSY at 500 Mz, $CDCl_3$/DMSO-d_6 (0.5 ml/0.2 ml)) ppm 26.49 (C^4), 28.84 (C^3), 29.07 (C^2), 38.41 (Phe^1–C$^{\beta}$–), 38.97 (C^1), 40.63 (Phe^2–C$^{\beta}$–), 53.52 (Phe^1–C$^{\alpha}$–), 56.17 (Phe^2–C$^{\alpha}$–), 126.35 (p^1-, p^2-), 128.00 (m^1-), 128.28 (m^2-), 129.17 (o^1-), 129.29 (o^2-), 137.17 (φ^2-), 137.97 (φ^1-), 170.62 (–NH^{b}CO–) and 173.90 (–NH^{a}CO–). IR (KBr) cm^{-1}; 3270 and 1640; *Anal.* Calcd for $C_{44}H_{48}N_6O_4$: C, 72.10; H, 7.70; N, 11.47. Found: C, 71.80; H. 7.72: N, 11.43.

Bis(L-Phe–D-Phe)-*N*,*N*-octane-1,8-diamine (19c) 70% yield: *Rf* (B) 0.31, mp 164—166 °C (from ether/$CHCl_3$). ^{1}H-NMR (signal assignments from the spectra of H–H COSY at 500 MHz, $CDCl_3$/DMSO-d_6 (0.5 ml/0.2 ml)) δ: 1.14—1.26 (m, 8H, –CH$_2$–CH$_2$–×2), 1.35—1.40 (m, 4H, –CH$_2$–×2), 2.53 (dd, 2H, *J*=8.85, 13.4 Hz, Phe^2–CH–×2), 2.86 (dd, 2H, *J*=7.6, 13.7 Hz, Phe^1–CH–×2), 2.94 (dd, 2H, *J*=4.6, 13.4 Hz, Phe^2–CH–×2), 2.98 (dd, 2H, *J*=6.1, 13.7 Hz, Phe^1–CH–×2), 3.02—3.13 (m, 4H, –CH$_2$–NHCO–×2), 3.46 (dd, 1H, *J*=4.6, 8.85 Hz, Phe^2–C$^{\alpha 2}$H–×2), 4.57 (ddd, 1H, *J*=7.6, 8.5, 14.0 Hz, Phe^1–C$^{\alpha 1}$H–×2), 7.12—7.21 (m, 8H, 4H×2, o^1-, o^2-), 7.17—7.18 (m, 4H, 2H×2, *p*-), 7.21—7.24 (m, 8H, 4H×2, *m*-), 7.70 (t, 2H, *J*=5.8 Hz, –NH^{a}CO–×2), and 8.03 (d, 2H, *J*=8.5 Hz, –NH^{b}CO–×2). ^{13}C-NMR (signal assignments from the spectra of C–H COSY at 500 Mz, $CDCl_3$/DMSO-d_6 (0.5 ml/0.2 ml) ppm 26.45 (C^4), 28.81 (C^3), 29.04 (C^2), 38.34 (Phe^1–C$^{\beta}$–), 38.81 (C^1), 40.95 (Phe^2–C$^{\beta}$–), 53.80 (Phe^1–C$^{\alpha}$–), 56.11 (Phe^2–C$^{\alpha}$–), 126.12 (p^1-), 126.24 (p^2-), 127.94 (m^1-), 128.10 (m^2-), 129.18 (o^1-), 129.21 (o^2-), 137.41 (φ^2-), 138.33 (φ^1-), 170.60 (–NH^{b}CO–) and 173.89 (–NH^{a}CO–). IR (KBr) cm^{-1}; 3270 and 1650; FAB-MS (NBA) *m/z* 725 (M+H)$^+$.

Bis(D-Phe–D-Phe)-*N*,*N*-octane-1,8-diamine (19d) 72% yield: *Rf* (B) 0.43; mp 171—171.5 °C; FAB-MS (NBA) *m/z* 725 (M+H)$^+$.

Bis(Dns–L-Phe)-*N*,*N*-ethane-1,2-diamine (21) Compound **6a** (0.128 g, 0.362 mmol) and dansyl chloride (Dns–Cl) (0.200 g, 0.742 mmol) was dissolved in 20 ml of acetone at room temperature and was stirred overnight. The solution was evaporated and the residue was extracted with ethyl acetate. The organic layer was washed with 5% $NaHCO_3$ and was combined, dried over $MgSO_4$, filtered, and concentrated under vacuum. The residue was purified by column chromatograhy on silica gel (100 mesh): *Rf* (B) 0.70, mp 114—117; HR-FAB-MS (NBA) Found 821.3163, Calcd for $C_{44}H_{48}N_6O_2S_2$ 821.3155.

CD Measurements The CD spectra of **18a**—**d** were measured on a JASCO J-600 spectrophotometer. Measurements were made in a 1 cm path length in 85% methanol, circular quartz cell at ambient temperature. The CD spectra are shown in Fig. 1 with molar ellipticity, [θ], *versus* wavelength, λ (nm).

Fluorescence Microscopy A431 cells (3×10^2 cells/ml) were cultured on 12-well plates and incubated for 24 h with 20 μl of 27.5 μg/ml and 3.5 μg/ml fluorescent labeling compound **21** in DMEM containing 10% fetal bovine serum (FBS) at 37 °C under a humidified 5% CO_2 atmosphere. At the end of the incubation, the cells were washed with PBS (−) and examined using an Olympus IX70 fluorescence microscope. At an excitation wavelength of 349 nm (λ_{ex}), compound **21** emits near wavelength of 530 nm (λ_{em}) in 85% methanol.

MIC and MBC Determination The minimum concentration for inhibition (MIC, μg/ml) was determined by the two-fold broth dilution method recommended by the Japan Society of Chemotherapy with a cation-supple-

mented Mueller-Hinton broth (CSMHB, pH=7.4).[15] A 50% dimethyl sulfoxide (DMSO) solution of the compound was diluted with CSMHB to an appropriate concentration. To 96-well plates was added 100 μl of the dilute compound solution. Bacterial suspensions for inocula, prepared by diluting overnight cultures to give a final concentration of 10^7 CFU/ml, and 5 μl of an inoculum, corresponding to about 5.0×10^4 CFU, was inoculated on the drug-containing wells. The 96-well microplates were incubated for 24 h at 37 °C. MIC was defined as the lowest concentration of the compound that prevented visible growth of the bacteria.

References

1) Hopkins R. B., Hamilton A. D., *J. Chem. Soc.*, *Chem. Commun.*, **1987**, 171—173 (1987).
2) Diaz H., Tsang K. Y., Choo D., Espina J. R., Kelly J. W., *J. Am. Chem. Soc.*, **118**, 3790—3791 (1996).
3) Nowick J. S., Holmes D. L., Mackin G., Noronha G., Shaka A. J., Smith E. M., *J. Am. Chem. Soc.*, **118**, 2764—2765 (1996).
4) Nesloney C. L., Kelly J. W., *Bioorgan. Med. Chem.*, **4**, 739—766 (1996).
5) Austin R. E., Maplestone R. A., Sefler A. M., Liu K., Hruzewicz W. N., Liu C. W., Cho H. S., Wemmer D. E., Bartlett P. A., *J. Am. Chem. Soc.*, **119**, 6461—6472 (1997).
6) Raghothama S. R., Awasthi S. K., Balaram P., *J. Chem. Soc.*, *Perkin Trans. 2*, **1998**, 137—143 (1998).
7) Kobayashi S., Kobayashi H., Yamaguchi T., Nishida M., Yamaguchi K., Kurihara M., Miyata N., Tanaka A., *Chem. Pharm. Bull.*, **48**, 920—934 (2000).
8) Wuthrich K., "NMR of Proteins and Nucleic Acids," John Wiley & Sons, New York, 1986.
9) Dyson H. J., Cross K. J., Houghten R. A., Wilson I. A., Lerner R. A., *Nature* (London), **318**, 480—487 (1985).
10) Ghose A. K., Pritchett A., Crippen G. M., *J. Comput. Chem.*, **9**, 80—90 (1988).
11) Matsuda H., Sato N., Tokunaga M., Naruto S., Kubo M., *Natural Medicines*, **56**, 113—116 (2002).
12) Merrifield R., Sahl H., Natori S., Elsbach P., Jacob L., Zasloff M., Flajnik M., Gabay J., Bevins C., "Antimicrobial Peptides" John Wiley & Sons, Chichester, 1996.
13) Matsuzaki K., Murase O., Fujii N., Miyajima K., *Biochemistry*, **34**, 6521—6526 (1995).
14) Grynkiewicz G., Poenie M., Tsien Y., *J. Biol. Chem.*, **260**, 3440—3450 (1985).
15) Japan Society of Chemotherapy, *Chemotherapy*, **41**, 184—189 (1993).